Extremely Bright Full Color Alternating Current Electroluminescence of Solution-Blended Fluorescent Polymers with Self-Assembled Block Copolymer Micelles

Sung Hwan Cho,[†,∥] Seong Soon Jo,[†,∥] Ihn Hwang,[†] Jinwoo Sung,[†,#] Jungmok Seo,[‡] Seok-Heon Jung,[§] Insung Bae,[†] Jae Ryung Choi,[†] Himchan Cho,[⊥] Taeyoon Lee,[‡] Jin Kyun Lee,[§] Tae-Woo Lee,[⊥] and Cheolmin Park[†,*]

[†]Department of Materials Science and Engineering, Yonsei University, Seoul 120-749, Republic of Korea, [‡]Department of Electrical and Electronic Engineering, Yonsei University, Seoul 120-749, Republic of Korea, [§]Department of Materials Science and Engineering, Inha University, Inchon 790-784, Republic of Korea, and [⊥]Department of Materials Science and Engineering, Pohang University of Science and Technology (POSTECH), Pohang 790-784, Republic of Korea. [∥]These authors contributed equally. [#]Present address: Dr. J. W. Sung, Materials and Devices Laboratory, LGE Advanced Research Institute, LG Electronics, 38 Baumoe-ro, Seocho-gu, Seoul 137-724, Korea.

ABSTRACT Electroluminescent (EL) devices operating at alternating current (AC) electricity have been of great interest due to not only their unique light emitting mechanism of carrier generation and recombination but also their great potential for applications in displays, sensors, and lighting. Despite great success of AC–EL devices, most device properties are far from real implementation. In particular, the current state-of-the art brightness of the solution-processed AC–EL devices is a few hundred candela per square meter (cd m^{-2}) and most of the works have been devoted to red and white emission. In this manuscript, we report extremely bright full color polymer AC–EL devices with brightness of approximately 2300, 6000, and 5000 cd m^{-2} for blue (B), green (G), and red (R) emission, respectively. The high brightness of blue emission was attributed to individually networked multiwalled carbon nanotubes (MWNTs) for the facile carrier injection as well as self-assembled block copolymer micelles for suppression of interchain nonradiative energy quenching. In addition, effective FRET from a solution-blended thin film of B-G and B-G-R fluorescent polymers led to very bright green and red EL under AC voltage, respectively. The solution-processed AC–EL device also worked properly with vacuum-free Ag paste on a mechanically flexible polymer substrate. Finally, we successfully demonstrated the long-term operation reliability of our AC–EL device for over 15 h.

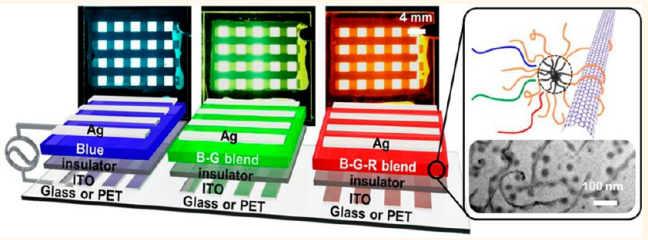

KEYWORDS: field-induced electroluminescence · FRET assisted AC electroluminescence · multiwalled carbon nanotubes · block copolymer micelles · fluorescent polymer · full color AC electroluminescence

Electroluminescent (EL) devices based on alternating current (AC) electric fields have a long-standing history with great potential for applications in displays, sensors, and lighting.[1−12] Numerous previous works have categorized the fundamental light-emitting mechanisms of devices by two main factors: solid-state cathode luminescence (SSCL)[1,2] and field-induced luminescence.[3,4] With SSCL, the impact excitation of the emitting layer is responsible for electroluminescence by hot electrons accelerated through an inorganic oxide layer. With field-induced luminescence, bipolar charges are sequentially injected from electrodes in an AC field and emit light upon recombination. Significant progress has been made to improve device performance for practical implementation, including developments in low driving voltage,[5,6] high brightness,[7,8] high power efficiency,[9] efficient color control and color mixing.[10]

AC–EL devices are readily fabricated with solution-processed and printable materials such as fluorescent polymers, self-assembled

* Address correspondence to cmpark@yonsei.ac.kr.

Received for review August 5, 2013 and accepted November 26, 2013.

Published online November 26, 2013
10.1021/nn4040926

inorganic/organic micelles and colloidal semiconducting quantum dots (QDs), which have been extensively studied in conventional DC mode EL devices.[11−13] Recent developments in emerging displays, lighting sources, and illumination sources are notable due to simple device architecture and low production costs.[8,14,15] Despite great success, most device properties are far from real implementation and the devices are not competitive with conventional DC mode polymer or QD light emitting devices.[16−19] In particular, the current state-of-the art brightness of the solution-processed AC−EL devices is a few hundred candela per square meter (cd m^{-2}) and most of the works have been devoted to red, green, and white emission.[5,6,10,20] One way to increase market availability of an AC−EL device is by discovering efficient routes for significantly improving the brightness of full blue (B), green (G), and red (R) colors.

Here, we report an extremely high brightness of solution-processed full color polymer AC−EL device with brightness of approximately 2300, 6000, and 5000 cd m^{-2} for blue, green, and red emission, respectively. Two novel strategies were employed to ensure high brightness: (1) AC driven fluorescence resonance energy transfer (FRET) was used between fluorescent polymers with different colors[21−24] and (2) self-assembled block copolymer micelles were incorporated as dilute agents to restrict the interchain interaction of fluorescent polymers.[25−27] The efficient long-range FRET of solution-blended BGR fluorescent polymers synergistically occurred while interchain nonradiative fluorescent quenching was suppressed by insulating nanometer scale micelles. This gave rise to high brightness of full color emission that was approximately 10 times greater than the brightness previously reported with solution-processed devices.[5,7,10] Furthermore, the high emission device platform with a simple and stacked metal/insulator/solution-processed emission layer and metal architecture was suitable with a mechanically flexible polymer substrate or a printable metal paste.

RESULTS AND DISCUSSION

The AC−EL device was fabricated by consecutively stacking four layers from bottom to top on transparent substrate that included an indium tin oxide (ITO) bottom electrode, insulator, solution-processed emission layer, and top electrode, as schematically shown in Figure 1a. The emission layer is a nanocomposite of three different components: fluorescent polymer, multiwalled carbon nanotubes (MWNTs) as facile carrier injection materials and block copolymer micelles as interchain diluting agents as well as agents for efficient dispersion of CNTs.[28,29] To utilize FRET between two fluorescent polymers, various combinations of three representative BGR polymers of blue poly spiro-bifluorene based copolymer, green F8BT, and red poly spiro-copolymer were made.

Highly dispersed MWNTs with poly(styrene-*block*-4vinylpyridine) (PS-*b*-P4VP) micelles in toluene were homogeneously mixed with fluorescent polymers. Subsequent spin coating of the solution resulted in an approximately 500-nm thick uniform nanocomposite layer with networked metallic MWNTs, as shown in a cross-sectional view of the composite in Figure 1b. In our previous work,[28] we have extensively investigated the effect of PS-*b*-P4VP micelles on dispersion of single walled carbon nanotubes with various experimental parameters such as concentration of micelles, micelle to CNT ratio, sonication time and solvents. The stability of the dispersion of a CNT solution was characterized by time-dependent UV−visible spectrum change. We have also examined the dispersion of MWNTs with the micelles and the results were very similar to those with SWNTs. All the solutions we used in the work were very stable in dispersion over long period of time longer than 5 days. Excellent MWNT dispersion with block copolymer micelles was attributed to the physical adhesion of micelles on the surface of nanotubes in which nonpolar PS blocks preferentially wrapped onto nanotubes,[28] as shown in Figure 1c (also see Supporting Information, Figure S1a). It should be, however, noted that the efficient dispersion of carbon nanotubes with block copolymer micelles has not been clearly understood yet. Based on our previous works,[28] we believe that the PS blocks, comprised by the corona of a micelle, wrapped themselves onto surface of SWNTs provided a good SWNT dispersion without alteration of chemical properties of nanotubes. The micelle absorption on the nanotubes was similarly observed previously in a model system with a polystyrene-*block*-polyethylene oxide (PS-*b*-PEO) copolymer on dielectric surfaces from a PS selective solvent, cyclohexane.[30] The study showed that above the critical micelle concentration (CMC), micelle adsorption was dominant and that the micelles were absorbed with the PS chains screening the attraction between the PEO blocks and the surface. Since the concentration of our PS-*b*-P4VP solution (0.5 wt %) is well above CMC of the block copolymer, our speculation is very plausible of the dispersion and stabilization of MWNTs in toluene by the PS-*b*-P4VP micelles whose PS corona blocks are physically absorbed on surface of the MWNTs with screening the attraction between P4VP and the nanotube surface as depicted in the schematic of Figure 1a.

The surface morphology of BGR blend films with block copolymer micelles and MWNTs in Figure 1d and the inset shows that micelles are preferentially associated with nanotubes on the film surface (also see Supporting Information, Figure S1b). In addition, individual or small aggregates of excess micelles that are not directly in contact with MWNTs are thoroughly distributed in the fluorescent polymer matrix. The surface profile of a height contrast image included in Supporting Information, Figure S1b showed its RMS roughness

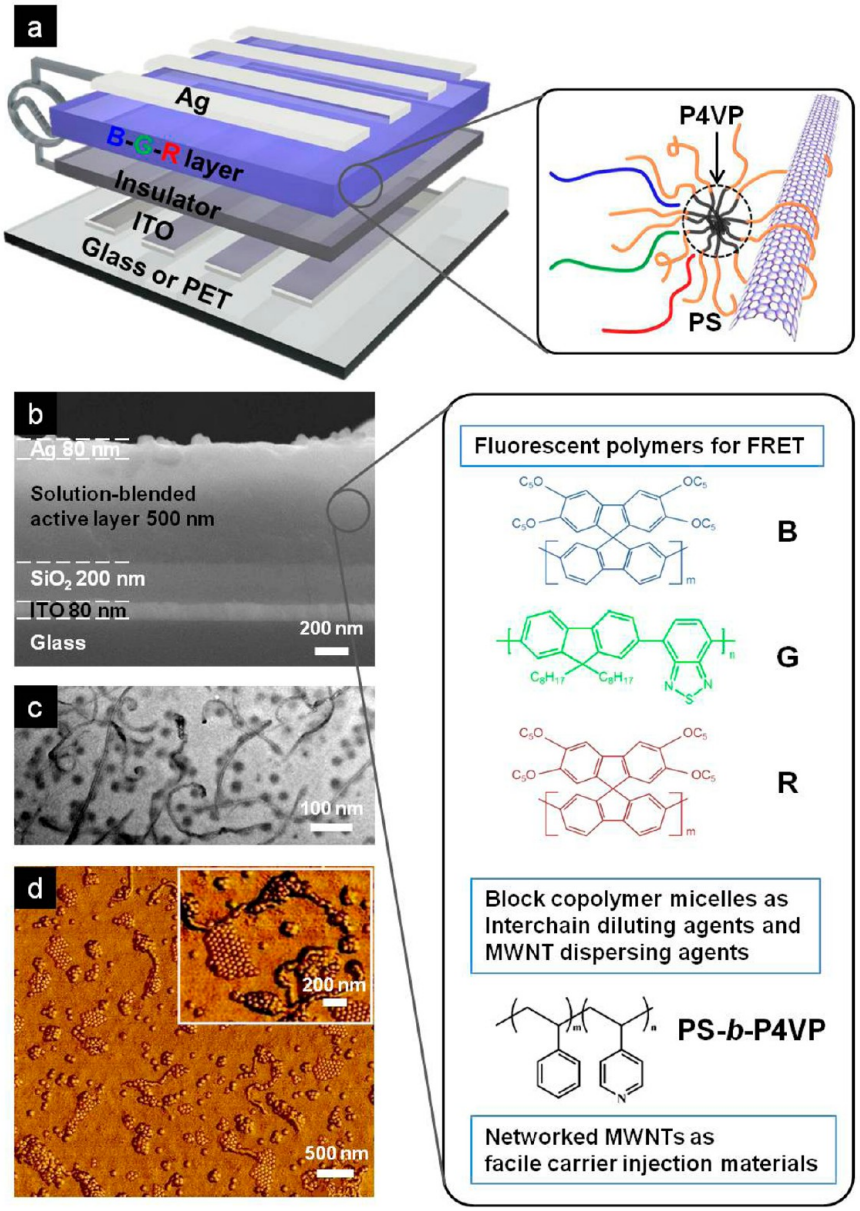

Figure 1. (a) Schematic of BGR blended AC−EL device fabricated by consecutive stacking of four layers composed of ITO/insulator/emitting layer/Ag electrode. Emitting layer includes solution processed fluorescent B, G, and R polymer and MWNTs self-assembled with PS-b-P4VP block copolymer micelles as highlighted on the box at the right. (b) SEM image of cross-sectional view of AC−EL device. Molecular structures of blue poly spiro-bifluorene based copolymer, green F8BT and red poly spiro-copolymer as fluorescent polymer. PS-*b*-P4VP micelles are shown on the right box. The detailed molecular structures of both blue and red polymers were not available from the manufacturer. (c) Bright field TEM image of nanostructure of solution-processed fluorescent polymer with MWNTs and PS-*b*-P4VP micelles. MWNTs were decorated with PS-*b*-P4VP micelles in which PS coronas preferentially wrapped themselves on nanotubes. (d) TM-AFM image shows MWNTs decorated with PS-*b*-P4VP micelles and free micelles uniformly distributed on the emitting layer surface. The inset shows a magnified image of (d).

of approximately 6 nm, which implies that the extra micelles aggregated on the surface of a nanocomposite rarely ruin the surface smoothness. It should be also noted that Figure 1d is the surface microstructure of a thin composite film employed to an AC−EL device while Figure 1c was obtained from a drop cast film from a highly diluted solution to visualize the assembly of PS-*b*-P4VP micelles on the nanotubes. The development of well dispersed nanotube networks, in which holes and electrons are readily injected from the top electrode to fluorescent polymer, is crucial. Too many nanotubes in a composite may result in aggregates, giving rise to significant nonradiative EL quenching. To achieve PS-*b*-P4VP micelles with an optimized amount of MWNTs, we prepared a nanocomposite with a blend ratio of fluorescent polymer to micelle of 4 to 1. This nanocomposite contained approximately 2 wt % MWNTs with respect to polymer.

Luminance−voltage (*L*−*V*) characteristics of single component AC−EL devices clearly show that the light

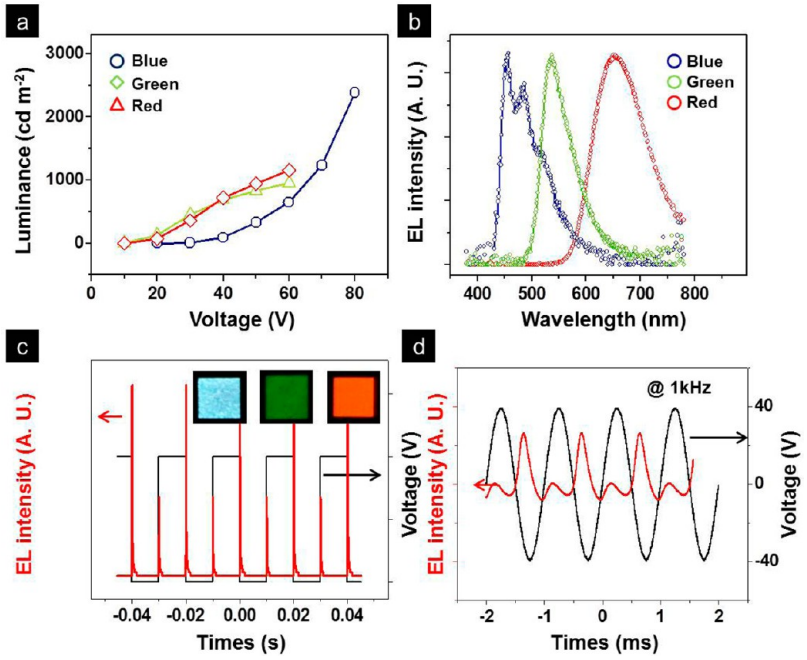

Figure 2. (a) Luminance−voltage (L−V) characteristics of single Blue, Green, and Red AC−EL devices at an AC frequency of 400 kHz with concentrations of MWNTs and PS-*b*-P4VP at 2 and 20 wt % with respect to nanocomposite, respectively. (b) Normalized EL spectra of the AC−EL devices with individual B,G and R fluorescent polymer mixed with MWNTs/PS-*b*-P4VP nanocomposites. The time-resolved EL signals of a red emitting AC−EL device (c) under successive ±110 V square-pulsed voltage trains with the frequency of 50 Hz (d) under successive ±40 V sinusoidal voltage inputs with the frequency of 1 kHz. The inset of (c) shows EL photograph of blue, green, and red light emission from the single component AC−EL devices operating at ±110 V and 50 Hz.

intensity of each device increased with applied voltage. The maximum EL intensities of B, G, and R polymer at an AC frequency of 400 kHz were 2380 cd m^{-2} at ±80 V, 950 cd m^{-2} at ±60 V, and 1150 cd m^{-2} at ±60 V, respectively, as shown in Figure 2a. Very weak luminescence was observed without carbon nanotubes and the luminescence was greatly enhanced with MWNTs up to a concentration of approximately 2 wt % in a nanocomposite above which EL tended to slightly decrease. (Supporting Information, Figure S2) The normalized EL spectra of single component AC−EL devices with MWNTs in Figure 2b exhibited maximum EL emission wavelengths at 480, 530, and 650 nm for blue, green, and red colors, respectively. This data is consistent with the photoluminescence (PL) spectra (Supporting Information, Figure S3). In particular, the highly bright blue emission of 2380 cd m^{-2} is notable and attributed to the MWNTs dispersed better in the blue polymer than other red and green one.

Extra PS-*b*-P4VP micelles that are blended with fluorescence polymers and not associated with MWNTs can enhance device brightness due to a diluting effect between fluorescent polymer chains with hairy PS corona blocks. To confirm this speculation, the amount of PS-*b*-P4VP micelles in nanocomposites was varied. The results clearly show that maximum AC−EL device brightness increased with PS-*b*-P4VP micelles. (Supporting Information, S4-a) Electrically insulating micelles also increased operating voltage while providing the good thermal stability of a composite film that is sustainable at high voltage as consistent with the results observed in conventional DC mode devices.[25] This trade-off between brightness and operation voltage requires an optimization of the amount of an insulator. Addition of PS homopolymer at a nanocomposite with a fixed PS-*b*-P4VP also resulted in the improvement of the brightness, which further supports the role of the extra block copolymer as diluting agents (Supporting Information, Figure S4b).

Temporal behavior of the emitted light in an AC EL clearly exhibited light emission at both polarities when driven by square-pulsed ±110 V at 50 Hz as shown in Figure 2c. The results indicate the sequential injection from top electrode to MWNTs and subsequent transfer of carriers to fluorescent polymer in which the formed excitons gave rise to light emission as consistent with our previous results with single wall carbon nanotubes.[5] As AC frequency increased, two distinct emissions at each polarity began to merge with each other and finally a very bright constant light emission independent of frequency was observed above 50 kHz (Supporting Information, Figure S5). The similar temporal behavior was also observed with sinusoidal voltage input required for power efficiency measurement as shown in Figure 2d (also see Supporting Information, Figure S6). Another important note is that the high brightness of our R, G, and B device made it feasible to directly operate at a condition similar to

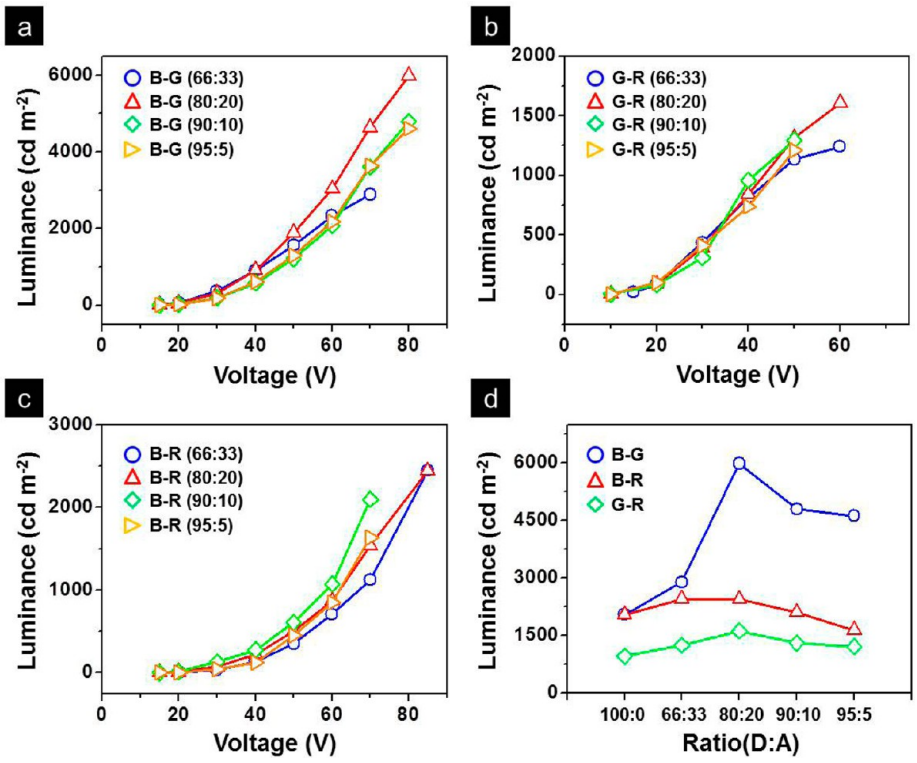

Figure 3. Light emission characteristics of FRET assisted AC–EL devices at an AC frequency of 400 kHz. All the devices examined include 2 and 20 wt % MWNTs and PS-*b*-P4VP micelles with respect to nanocomposite, respectively. Luminance–Voltage characteristics of AC–EL devices containing (a) B-G, (b) G-R, and (c) B-R binary mixtures with different blend compositions. (d) Plots of maximum luminance values of the binary B-G, B-R, and G-R blends as a function of the mixing compositions of two polymers.

in-house AC electric condition, *i.e.*, 110 V_{RMS} at 50 Hz, although its brightness was significantly reduced due to insufficient hole and electron carriers as shown in the inset of Figure 2c.

Further enhancement of green and red brightness was achieved by FRET between donor and acceptor polymer. The absorbance spectra and photoluminescence spectra of B, G, and R polymer films suggest that an excited blue molecule arising from AC operation transfers its energy to green polymer and both excited blue and green molecule transferred to red molecule (Supporting Information, Figure S3). This is followed by green and red PL emission, leading to extremely bright FRET driven AC–EL. Significantly improved AC green EL was obtained with brightness of approximately 6000 cd m^{-2} in an AC EL device containing a mixture of blue-green polymers (D-A = 8:2) as shown in Figure 3a. Thorough investigation of various blend compositions of B-G, B-R, and G-R allowed for optimized blend compositions giving rise to enhanced green and red emission, as shown in Figure 3. The maximum luminance of the binary B-G, B-R, and G-R blends as a function of the mixing compositions of two polymers are shown in Figure 3d (also see Supporting Information, Figure S7).

To further increase the brightness of AC red emission, we utilized cascade FRET between BGR polymers from a ternary mixture of B, G, and R polymers as shown in Figure 4a. An optimum blend composition of B, G, and R polymers was determined with 0.5, 0.25, and 0.25 weight fraction, respectively, and a device with the ternary blend emitted red light of approximately 3100 cd m^{-2}. The EL spectra of AC–EL devices with B, B-G, and B-G-R mixture exhibit characteristic emission peaks with maximum wavelengths of approximately 480, 530, and 640 nm, respectively as shown in Figure 4b. Their un-normalized, absolute intensities all comparable with each other can be beneficial for full color BGR generation. The Commission Internationale de l'Enclairage (CIE) coordinate of the devices obtained simultaneously with the EL spectra was (0.625, 0.373), (0.385, 0.577), and (0.156, 0.221), which corresponds to typical red, green, and blue emission, as shown in Figure 4c. In addition, the EL spectra exhibit no change with increasing the voltage, indicative of the high-quality BGR light emission. (Supporting Information, S8) Extremely bright B, G, and R emission from our AC EL devices working at the operating voltage of either 70 or 80 V and the frequency of 400 kHz are clearly visible in photographs of Figure 4d. All the EL characteristics of AC EL devices with different mixing ratio of the three polymers are summarized in Table 1.

It is also important to investigate the device efficiency, defined as the ratio of photometric power

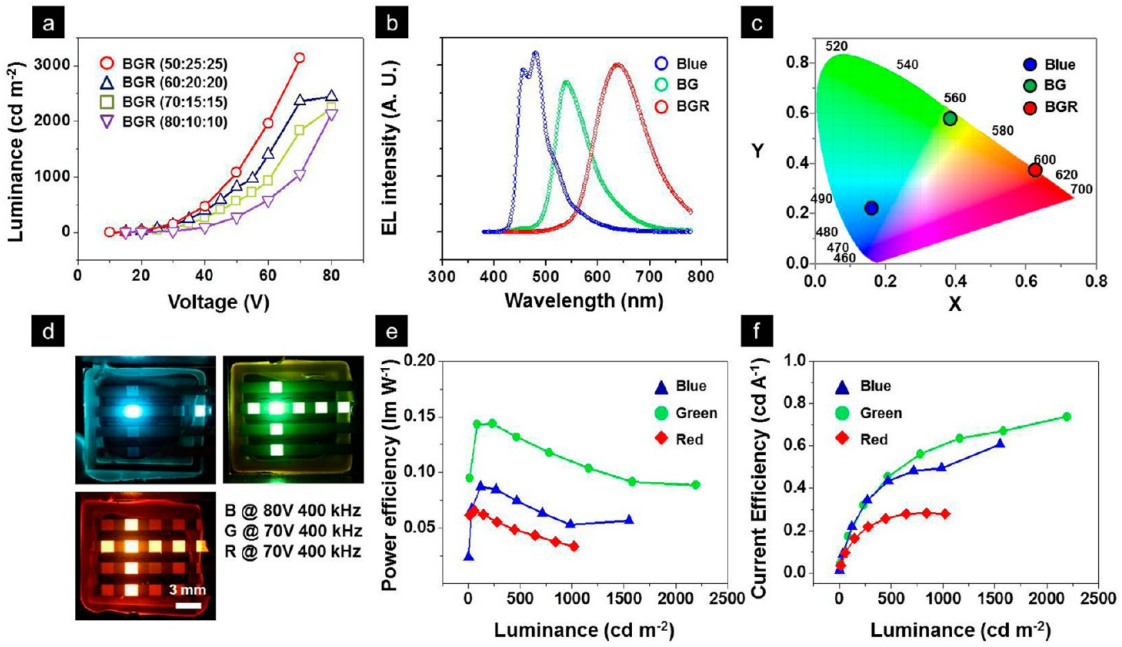

Figure 4. Light emission and efficiency characteristics of FRET assisted AC–EL devices. The devices examined include 2 and 20 wt % MWNTs and PS-*b*-P4VP micelles with respect to nanocomposite, respectively, at an AC frequency of 400 kHz (a–d) and 50 kHz (e–f). (a) Luminance–voltage (*L*–*V*) curves of red-emitting AC–EL devices assisted by cascade FRET between BGR polymers with different mixing ratio of the three polymers. (b) Un-normalized and absolute EL spectra of AC–EL devices with B, B-G, and B-G-R mixture AC EL devices. (c) Color space chromaticity diagram showing CIE coordinates of emitting light from B, B-G, and B-G-R AC–EL devices. (d) Photographs of extremely bright B, G, and R emission from B, B-G, and B-G-R AC–EL devices. (e) Luminous power efficiency and (f) current efficiency of B, B-G, and B-G-R AC–EL devices as a function of luminance. Sinusoidal voltage input with 50 kHz was applied.

TABLE 1. EL Characteristics for AC–EL Devices with Different Mixing Ratio of the Three Polymers

	ratio (%)	L_{max} (cd m^{-2})	V_{max} (V)	CIE coordinate (*x*,*y*)	λ_{peak} (nm)
R	R100	1153	60	(0.6466,0.3516)	650
G	G100	954	60	(0.4317,0.5542)	540
B	B100	2387	80	(0.1739,0.2562)	455
GR	G66:R33	1241	60	(0.6181,0.4792)	622
	G80:R20	1607	60	(0.6181,0.3792)	640
	G90:R10	1295	50	(0.6024,0.3940)	626
	G95:R5	1208	50	(0.5808,0.4136)	628
BG	B66:G33	2886	70	(0.4015,0.5652)	540
	B80:G20	5984	80	(0.3946,0.5615)	538
	B90:G10	4796	80	(0.3818,0.5667)	536
	B95:G5	4612	80	(0.3728,0.5666)	541
BR	B66:R33	2446	85	(0.6279,0.3698)	630
	B80:R20	2442	85	(0.6213,0.3752)	628
	B90:R10	2098	70	(0.6058,0.3865)	617
	B95:R5	1635	70	(0.5961,0.3880)	625
BGR	B50:G25:R25	3131	70	(0.6293,0.3682)	640

emitted from the device to the electrical input power. The input power per unit area in an AC EL device is calculated as a function of input voltage, current developed during operation and phase angle between sinusoidal voltage and current. The current of a device containing 200 nm thick insulating layer during AC operation is the displacement current through the capacitor arising from the charges built up on the plates of the capacitor. Although charge carriers are injected from the top electrode to an emitting nanocomposite layer, the DC driven current through the emitting layer was very low of approximately 10^{-6} A due to the dielectric layer and thus no light was emitted under DC bias. Above dielectric breakdown voltage of the dielectric layer, the device exhibited localized spikes due to the conduction paths developed between top and bottom electrode.[5] It should be noted that in this sense, the power efficiency of an AC–EL device is quite different from one of a conventional DC-EL one in principle, making it inappropriate to directly compare the efficiency of an AC device with that of DC one.

Luminous power efficiency in lumen per watt (lm W^{-1}) of our device was in the range from 0.05–0.15 for all BGR colors when sinusoidal voltage input with the maximum voltage of ±50 V was applied at 50 kHz as shown in Figure 4e (also see Supporting Information Figure S9). Power efficiency in general increased with applied voltage at a given frequency and decreased with frequency at a given voltage, consistent with the results from AC EL devices previously fabricated with vacuum process.[6,9] Our device also exhibited the characteristic AC frequency dependence of impedance, resistance, reactance and phase angle of a capacitive device (Supporting Information Figure S9). The power efficiency values of our BGR devices are slightly low, compared with those reported with vacuum-processed AC–EL devices containing elaborately stacked 9 layers. Perumal *et al.* demonstrated the

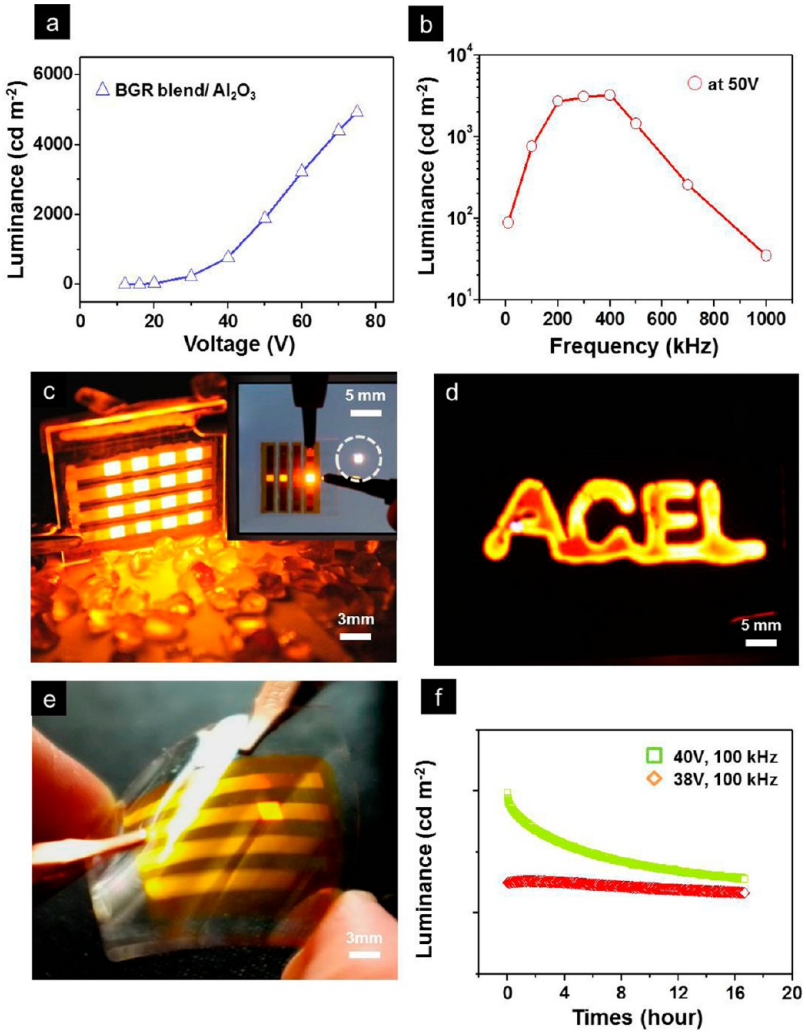

Figure 5. (a) Luminance−voltage (*L*−*V*) characteristics of a BGR blended AC−EL device at 400 kHz fabricated on a high k Al_2O_3 insulator. (b) Luminance−f requency plot of the BGR blended AC−EL device at ±50 V. (c) Photographs of red light emission from BGR blended AC−EL device with Al_2O_3 insulator. Inset shows comparison of our device with area-corrected smart phone display. (d) Photograph of red light emission under hand-written letters of Ag paste top electrode. (e) Photograph of BGR blended AC−EL device fabricated on mechanically flexible PET substrate under bending radius of approximately 15 mm. (f) Brightness−operation time plot of BGR blended AC−EL device. In all devices, Ag top electrode was used and the concentrations of PS-*b*-P4VP and MWNTs were 20 and 2 wt % with respect to nanocomposite, respectively.

maximum efficiency of 0.37 lm W^{-1} of an AC EL device[6] and recently they further optimized both driving voltage and frequency to develop a device with its power efficiency of 2.7 lm W^{-1} at 2 kHz.[9] We believe that the efficiency of our device is, however, still notable since it has a simple and stacked 4 layer architecture with an emitting layer of solution-processed polymer nanocomposite. The maximum luminous efficiency at 1000 cd m^{-2} of our devices is approximately 0.6 cd A^{-1} for a green device as shown in Figure 4f. More systematic investigation is under way for improving the device efficiency.

Further optimization of the brightness of an AC EL device was made by properly selecting insulator material. The device emitted enhanced EL even with turn-on threshold voltage that was lower when SiO_2 ($k \sim 3.9$) insulator was replaced by a high k Al_2O_3 ($k \sim 9$) insulator[31,32] prepared by atomic layer deposition. This was due to more plentiful charge accumulation than with SiO_2. The brightness of a FRET induced, red-emitting AC− EL device with BGR mixture was further improved to approximately 5000 cd m^{-2}, as shown in Figure 5a,b. Full operation of 16 device cells with 2×2 mm^2 emitting areas each gave rise to sufficient brightness for illumination, as shown in Figure 5c. The device's brightness was also confirmed by comparing it with a commercially available area-corrected smart phone display, as shown in the inset of Figure 5c.

Solution-processed nanocomposites can be used for versatile applications. For instance, conventional Ag paste top electrodes were directly written on the blended composite, giving rise to light emission on hand-written letters of Ag paste, as shown in Figure 5d. In addition, an AC−EL device was conveniently fabricated on mechanically flexible poly(ethylene terephthalate) substrate on which ITO, polymer insulator, and active BGR composite layer were sequentially deposited.

This was followed by thermal deposition of a top Ag electrode, as shown in Figure 5e. The device emitted bright red light under AC conditions, but its brightness reduced to approximately 500 cd m^{-2} due to nonuniformity of the plastic substrate. This resulted in local breakdown of the device at high AC voltage. The device operated properly at bending deformation with a bending radius of approximately 15 mm. Furthermore, the FRET induced AC–EL device exhibited excellent emission reliability when it was encapsulated with an epoxy resin that protected fluorescent polymers from oxygen and water molecules. An initial brightness of approximately 100 cd m^{-2} gradually decreased with time to 50 cd m^{-2} after 7 h, as shown in Figure 5f. When driving voltage decreased slightly, the initial brightness of approximately 30 cd m^{-2} was not altered with long operation time, as shown in Figure 5f .

CONCLUSIONS

We demonstrated extremely bright full color polymer AC–EL devices with solution processed emissive nanocomposites of fluorescent polymer, self-assembled block copolymer and MWNTs. The high brightness of blue emission of approximately 2300 cd m^{-2} was attributed to individually networked MWNTs for the facile carrier injection and transfer as well as self-assembled block copolymer micelles for not only efficient dispersion of MWNTs but also suppression of inter-chain nonradiative energy quenching. Furthermore, effective long-range fluorescent energy transfer from a blended thin film of B-G and B-G-R fluorescent polymers led to very bright green and red EL of approximately 6000 and 5000 cd m^{-2} under AC operation, respectively, considering that the current state-of-the art brightness of the solution-processed AC–EL devices is a few hundred candela per square meter. The solution-processed AC–EL device also worked properly with vacuum-free Ag paste on a mechanically flexible polymer substrate. Finally, our device exhibited the long-term operation reliability of our AC–EL device for over 15 h. Our results offer a novel design strategy for not only AC driven display and lighting but also various emerging color contrast biological and chemical sensing devices.

METHODS

Materials. Green light-emitting fluorescent polymer, poly-[(9,9-di-*n*-octylfluorenyl-2,7-diyl)-alt-(benzo[2,1,3]thiadiazol-4,8-diyl)] (F8BT), was synthesized as previously described. A red poly spiro-copolymer (Product: SPR-001) and blue poly spiro-bifluorene based copolymer (Product: SPB-02T) were purchased from Merck Co. Multiwalled carbon nanotubes (MWNTs) (Grade: TMC220-10) purified over 95 wt % and grown by CVD were manufactured at Nano Solution, Inc., Seoul, Korea. Poly(styrene-*b*-vinyl pyridine) (PS-*b*-P4VP) was synthesized by Polymer Source, Inc., Doval, Canada. The molecular weight of PS and P4VP was 10 400 and 19 200 g mol^{-1}, respectively. The polydispersity index (PDI = M_w/M_n) of PS-*b*-P4VP was 1.27. All other materials were purchased from Aldrich and used for AC–EL devices without further purification.

Preparation of Fluorescent Polymer/PS-*b*-P4VP/MWNT Composites. A solution of 0.5 wt % PS-*b*-P4VP dissolved in toluene was prepared by stirring for 1 h at 80 °C. The 0.5 wt % PS-*b*-P4VP was used as a MWNT dispersant. Various amounts of MWNTs were dispersed in 0.5 wt % PS-*b*-P4VP solution with 1 to 3 wt % nanocomposite. The PS-*b*-P4VP to MWNT ratio was 10. Solution mixtures of PS-*b*-P4VP and MWNTs were bath-sonicated (NXP-1002, 60 Hz, 120 W, Kodo Technical Research Co., Ltd.) for 30 min followed by horn-sonication for 5 min (VC 750, Sonics & Materials, Inc.). In most of the cases, individual fluorescent polymers or mixtures of two or three polymers were directly dissolved into the well-dispersed MWNT solutions (0.5 mg/mL) with PS-*b*-P4VP (5 mg/mL), leading to a nanocomposite solution of a polymer (fluorescent/block copolymer) of 25 mg/mL.

AC–EL Device Fabrication. AC–EL devices were comprised of four layers of ITO/dielectric layer/emissive layer/metal electrode. AC–ELs were fabricated on glass substrate coated with prepatterned 2-mm-wide strips of transparent bottom electrodes consisting of indium tin oxide (ITO) with sheet resistance of ~10 Ω sq^{-1}. Insulating layers, such as SiO_2 and Al_2O_3, with the thickness of 200 nm were deposited onto ITO/glass substrates. SiO_2 layers were deposited onto the ITO surface with low-pressure plasma (10^{-5} Torr) at 400 °C using plasma-enhanced chemical vapor deposition purchased from Freemteck, Inc., South Korea. Al_2O_3 was deposited by atomic layer deposition (ALD) onto ITO in a laboratory. For a flexible AC–EL device, a thin poly(4-vinylphenol) (PVP) insulator was prepared by spin coating 5 wt % PVP solution with poly(melamine-*co*-formaldehyde) as a cross-linking agent (CLA) in a ratio of 1:1 by weight in propylene glycol monomethyl ether acetate (PGMEA). The film was subsequently cured at 150 °C for 30 min for cross-linking. Emissive composite layers were spin-coated using fluorescent polymer/PS-*b*-P4VP/MWNT solutions onto dielectric layers at 1000 rpm for 60 s followed by baking at 150 °C for a flexible EL device and 200 °C for a EL device on glass substrate for 30 min. These AC–EL devices were loaded into a high-vacuum thermal evaporator (Thermal Evaporator: MEP 5000, SNTEK Co., Ltd.) to deposit 2-mm-wide strips of Ag top electrodes through a shadow Sus-Mask under background pressure of ~3 × 10^{-7} Torr at a rate of 0.1 nm/s. Consequently, the completed AC-TFEL devices had active device areas of 2 × 2 mm^2 cells at the intersections of bottom and top electrode strips. AC-TFEL devices were powered by an Agilent 20 MHz function generator with a voltage amplifier.

Characterization. The nanostructures of blended fluorescent polymer/PS-*b*-P4VP/MWNTs were analyzed using a tapping mode atomic force microscope (AFM) (Nanoscope IV[a] Digital Instruments-) in height and phase contrast, a field-emission scanning electron microscope (FESEM) (JEOL JSM-600F), and a high-resolution transmission electron microscope (HRTEM) (JEOL 2100F) in bright field mode. The optical absorbance and fluorescence spectra for solutions and films were obtained using a JASCO V-530 UV visible spectrophotometer and a Varian Cary Eclipse fluorescence spectrophotometer, respectively. The brightness and electroluminescence spectra of devices were obtained with a spectroradiometer (Konica CS 2000). Temporal behavior of electroluminescence was measured using a silicon photodiode connected to oscilloscope (Agilent Infinium) with optical filter having approximately 50 nm passband centered at 550 nm. The current voltage and power efficiency measurement was carried out using multichannel precision power analyzer (ZIMMER electronics systems LMG 500). All measurements were done in a dark box at room temperature in air.

Conflict of Interest: The authors declare no competing financial interest.

Supporting Information Available: Optical images, SEM images, L–V, L–F data, and ACEL efficiency results. This material is available free of charge *via* the Internet at http://pubs.acs.org.

Acknowledgment. This project was supported by DAPA, ADD, and the Converging Research Center Program through the Ministry of Science, ICT and Future Planning, Korea (2013K000183), the National Research Foundation of Korea (NRF) grant funded by the Korea government (MSIP) (No. 2007-0056091), the Pioneer Research Center Program through the National Research Foundation of Korea funded by the Ministry of Science, ICT & Future Planning (2010-0019313). This work was supported by a Global Ph.D. Fellowship conducted by the National Research Foundation of Korea in 2013. This research was also supported by the Second Stage of the Brain Korea 21 Project in 2006 and the Korea Science and Engineering Foundation.

REFERENCES AND NOTES

1. Xu, X. L.; Chen, X. H.; Hou, Y. B.; Xu, Z.; Yang, X. H.; Yin, S. G.; Wang, Z. J.; Xu, X. R.; Lau, S. P.; Tay, B. K. Blue Electroluminescence from Tris-(8-hydroxyquinoline) Aluminum Thin Film. *Chem. Phys. Lett.* **2000**, *325*, 420–424.
2. Yang, S. Y.; Qian, L.; Teng, F.; Xu, Z.; Xu, X. R. Alternating-Current Electroluminescence from an Organic Heterojunction Sandwiched between Two Amorphous SiO_2 Layers. *J. Appl. Phys.* **2005**, *97*, 126101–126103.
3. Gu, G.; Parthasarathy, G.; Burrows, P. E.; Tian, P.; Hill, I. G.; Kahn, A.; Forrest, S. R. Transparent Stacked Organic Light Emitting Devices. I. Design Principles and Transparent Compound Electrodes. *J. Appl. Phys.* **1999**, *86*, 4067–4075.
4. Tsutsui, T.; Lee, S.; Fujita, K. Charge Recombination Electroluminescence in Organic Thin-Film Devices without Charge Injection from External Electrodes. *Appl. Phys. Lett.* **2004**, *85*, 2382–2384.
5. Sung, J.; Choi, Y. S.; Kang, S. J.; Cho, S. H.; Lee, T.-W.; Park, C. AC Field-Induced Polymer Electroluminescence with Single Wall Carbon Nanotubes. *Nano Lett.* **2011**, *11*, 966–972.
6. Perumal, A.; Fröbel, M.; Gorantla, S.; Gemming, T.; Lüssem, B.; Eckert, J.; Leo, K. Novel Approach for Alternating Current (AC)-Driven Organic Light-Emitting Devices. *Adv. Funct. Mater.* **2012**, *22*, 210–217.
7. Perumal, A.; Lüssem, B.; Leo, K. Ultra-Bright Alternating Current Organic Electroluminescence. *Org. Electron.* **2012**, *13*, 1589–1593.
8. Wang, Z. G.; Chen, Y. F.; Li, P. J.; Hao, X.; Liu, J. B.; Huang, R.; Li, Y. R. Flexible Graphene-Based Electroluminescent Devices. *ACS Nano* **2011**, *5*, 7149–7154.
9. Frobel, M.; Perumal, A.; Schwab, T.; Gather, M. C.; Lussem, B.; Leo, K. Enhancing the Efficiency of Alternating Current Driven Organic Light-Emitting Devices by Optimizing the Operation Frequency. *Org. Electron.* **2013**, *14*, 809–813.
10. Cho, S. H.; Sung, J.; Hwang, I.; Kim, R. H.; Choi, Y. S.; Jo, S. S.; Lee, T.-W.; Park, C. High Performance AC Electroluminescence from Colloidal Quantum Dot Hybrids. *Adv. Mater.* **2012**, *24*, 4540–4546.
11. Burroughes, J. H.; Bradley, D. D. C.; Brown, A. R.; Marks, R. N.; MacKay, K.; Friend, R. H.; Burn, P. L.; Holmes, A. B. Light-Emitting Diodes Based on Conjugated Polymers. *Nature* **1990**, *347*, 539–541.
12. Sun, Z.; Bai, F.; Wu, H.; Boye, D. M.; Fan, H. Monodisperse Fluorescent Organic/Inorganic Composite Nanoparticels. *Chem. Mater.* **2012**, *24*, 3415–3419.
13. Kim, T.-H.; Cho, K.-S.; Lee, E. K.; Lee, S. J.; Chae, J.; Kim, J. W.; Kim, D. H.; Kwon, J.-Y.; Amaratunga, G.; Lee, S. Y.; *et al.* Full-Colour Quantum Dot Displays Fabricated by Transfer Printing. *Nat. Photonics* **2011**, *5*, 176–182.
14. Wood, V.; Panzer, M. J.; Chen, J.; Bradley, M. S.; Halpert, J. E.; Bawendi, M. G.; Bulović, V. Inkjet-Printed Quantum Dot–Polymer Composites for Full-Color AC-Driven Displays. *Adv. Mater.* **2009**, *21*, 2151–2155.
15. Wood, V.; Panzer, M. J.; Bozyigit, D.; Shirasaki, Y.; Rousseau, I.; Geyer, S.; Bawendi, M. G.; Bulović, V. Electroluminescence from Nanoscale Materials *via* Field-Driven Ionization. *Nano Lett.* **2011**, *11*, 2927–2932.
16. Lee, T.-W.; Chung, Y.; Kwon, O.; Park, J.-J. Self-Organized Gradient Hole Injection to Improve the Performance of Polymer Electroluminescent Devices. *Adv. Funct. Mater.* **2007**, *17*, 390–396.
17. Fong, H. H.; Lee, J.-K.; Lim, Y.-F.; Zakhidov, A. A.; Wong, W. W. H.; Holmes, A. B.; Ober, C. K.; Malliaras, G. G. Orthogonal Processing and Patterning Enabled by Highly Fluorinated Light-Emitting Polymers. *Adv. Mater.* **2011**, *23*, 735–739.
18. Kwak, J.; Bae, W. K.; Lee, D.; Park, I.; Lim, J.; Park, M.; Cho, H.; Woo, H.; Yoon, D. Y.; Char, K. Bright and Efficient Full-Color Colloidal Quantum Dot Light-Emitting Diodes Using an Inverted Device Structure. *Nano Lett.* **2012**, *12*, 2362–2366.
19. Caruge, J.-M.; Halpert, J. E.; Wood, V.; Bawendi, M. G.; Bulović, V. Colloidal Quantum-Dot Light-Emitting Diodes with Metal-Oxide Charge Transport Layers. *Nat. Photonics* **2008**, *2*, 247–250.
20. Chen, Y.; Smith, G. M.; Loughman, E.; Li, Y.; Nie, W.; Carroll, D. L. Effect of Multi-Walled Carbon Nanotubes on Electron Injection and Charge Generation in AC Field-Induced Polymer Electroluminescence. *Org. Electron.* **2013**, *14*, 8–18.
21. Park, Y. H.; Kim, Y.; Sohn, H.; An, K.-S. Concentration Quenching Effect of Organic Light-Emitting Devices Using DCM1-Doped Tetraphenylgermole. *J. Phys. Org. Chem.* **2012**, *25*, 207–210.
22. Kan, S.; Liu, X.; Shen, F.; Zhang, J.; Ma, Y.; Zhang, G.; Wang, Y.; Shen, J. Improved Efficiency of Single-Layer Polymer Light-Emitting Devices with Poly(vinylcarbazole) Doubly Doped with Phosphorescent and Fluorescent Dyes as the Emitting Layer. *Adv. Funct. Mater.* **2003**, *13*, 603–608.
23. Bulovic, V.; Shoustikov, A.; Baldo, M. A.; Bose, E.; Kozlov, V. G.; Thompson, M. E.; Forrest, S. R. Bright, Saturated, Red-to-Yellow Organic Light-Emitting Devices Based on Polarization-Induced Spectral Shifts. *Chem. Phys. Lett.* **1998**, *287*, 455–460.
24. Dexter, D. L.; Schulman, J. H. Theory of Concentration Quenching in Inorganic Phosphors. *J. Chem. Phys.* **1954**, *22*, 1063–1070.
25. Kulkarni, A. P.; Jenekhe, S. A. Blue Light-Emitting Diodes with Good Spectral Stability Based on Blends of Poly(9,9-dioctylfluorene): Interplay between Morphology, Photophysics, and Device Performance. *Macromolecules* **2003**, *36*, 5285–5296.
26. He, G.; Li, Y. Enhanced Electroluminescence Using Polystyrene as a Matrix. *Appl. Phys. Lett.* **2002**, *80*, 4247–4249.
27. Burin, A. L.; Ratner, M. A. Exciton Migration and Cathode Quenching in Organic Light Emitting Diodes. *J. Phys. Chem. A* **2000**, *104*, 4704–4710.
28. Shin, H.; Min, B. G.; Jeong, W.; Park, C. Amphiphilic Block Copolymer Micelles: New Dispersant for Single Wall Carbon Nanotubes. *Macromol. Rapid Commun.* **2005**, *26*, 1451–1457.
29. Sung, J.; Jo, P. S.; Shin, H.; Huh, J.; Min, B. G.; Kim, D. H.; Park, C. Transparent, Low-Electric-Resistance Nanocomposites of Self-Assembled Block Copolymers and SWNTs. *Adv. Mater.* **2008**, *20*, 1505–1510.
30. Munch, M. R.; Gast, A. P. Kinetics of Block Copolymer Adsorption on Dielectric Surfaces from a Selective Solvent. *Macromolecules* **1990**, *23*, 2313.
31. Choi, J.-H.; Fafarman, A. T.; Oh, S. J.; Ko, D.-K.; Kim, D. K.; Diroll, B. T.; Muramoto, S.; Gillen, J. G.; Murray, C. B.; Kagan, C. R. Bandlike Transport in Strongly Coupled and Doped Quantum Dot Solids: A Route to High-Performance Thin-Film Electronics. *Nano Lett.* **2012**, *12*, 2631–2638.
32. Hwang, D. K.; Fuentes-Hernandez, C.; Kim, J.; Potscavage, W. J.; Kim, S.-J.; Kippelen, B. Top-Gate Organic Field-Effect Transistors with High Environmental and Operational Stability. *Adv. Mater.* **2011**, *23*, 1293–1298.